A SYNTHESIS BETWEEN EXPERIMENTAL AND NUMERICAL METHODS APPLIED TO THE DETERMINATION OF CRACK RESISTANCE CURVES FOR VARIOUS SPECIMENS

Dietmar Klingbeil[1], Georgia Künecke[1], Johannes Schicker[1]

Ductile fracture of ferritic steels is caused by the nucleation, growth and coalescence of voids. A model commonly used has been established by Gurson introducing the void volume fraction as a damage parameter. Several experiments have been carried out for notched bars, C(T), M(T) and statically loaded Charpy-V-notched specimens, all made of the same mild steel. Gurson's model was implemented into a finite element code and was applied to all those specimens assuming either axisymmetric or plane strain conditions. Several calculations were performed to model the behaviour of all specimens with one material parameter set, which was found to be independent from loading and geometry.

INTRODUCTION

One of the most important questions in fracture mechanics of ductile materials is, how results obtained from different fracture mechanics specimens depend on loading conditions and the geometry of the specimens and how to adopt results obtained from laboratory experiments on specimens to real structures. Much work has been done during recent years to explain the dependence of crack resistance curves on the geometry and loading conditions of specimens using global concepts but a general concept, which material parameters are loading and geometry independent and should be used, is still missing.

One method to obtain loading and geometry independent material parameters is to model the microscopic process of ductile crack growth, which consists of the nucleation, growth and coalescence of voids. This process is described by constitutive equations, which are implemented into finite element codes allowing the

[1]Federal Institute for Materials Research and Testing (BAM),
Unter den Eichen 87, D-12205 Berlin, Federal Republic of Germany

simulation of ductile tearing even without the presence of an initial crack. The application of such models usually requires a hybrid methodology where the material parameters of the model are determined by the numerical simulation of the experiments. A model commonly used was introduced by Gurson (1) and modified by Needleman and Tvergaard (2). In the present investigation, this model is taken for the simulation of experiments on notched tensile bars from which the material parameters are determined. In a subsequent step, the stable crack growth in C(T), M(T) and statically loaded Charpy-V-notched specimens is simulated taking the identical material parameters, where all specimens are made of a mild steel with the German designation StE 460.

CONSTITUTIVE EQUATIONS

Most engineering metals are ductile and contain rigid inclusions or second-phase particles. Under an increasing load, a debonding process occurs at the interfaces between the inclusions and the ductile matrix which causes damage represented by voids or microcracks. A further loading in the plastic regime results in growth and coalescence of voids. Constitutive equations taking the micromechanical process of ductile void growth into account base on considerations of simple unit cell models with a mostly spherical cavity in a surrounding ductile matrix. Such investigations were performed by McClintock (3) and Rice and Tracey (4), who all found an exponential dependence of the void growth rate from the stress triaxiality σ_h/σ_e. Rice and Tracey (4) found the evolution equation for a cavity with radius R in a perfectly plastic matrix as

$$\frac{\dot{R}}{R} = 0.283\ \dot{\varepsilon}^p\ e^{\frac{3\sigma_h}{2\sigma_e}} \quad . \tag{1}$$

with $\dot{\varepsilon}^p$ being the rate of the plastic accumulated strain, σ_h is the hydrostatic part of the stress tensor, and σ_e is the effective stress, respectively. Eqn. (1) was adopted by Gurson (1), who developed a yield condition for a spherical cavity in a perfectly plastic matrix, where yielding even occurs, if only the hydrostatic part $tr\,\underline{T}$ of the stress tensor $\underline{T}$ is active, which is in contrast to the conventional v. Mises plasticity:

$$\Phi(\underline{T}', tr\underline{T}, f, \sigma_m) = \frac{3\,\underline{T}' \cdot\cdot\, \underline{T}'}{2\sigma_m^2} + 2f\cosh\left(\frac{tr\underline{T}}{2\sigma_m}\right) - 1 - f^2 \quad . \tag{2}$$

The deviatoric part of the stress tensor is denoted $\underline{T}'$, and the void volume fraction f is defined as the ratio of the void volume to the whole volume of a unit cell. Gurson's yield condition was modified by Tvergaard and Needleman (2), who introduced an empirical parameter q, which takes account to the fact, that failure of

a unit cell does not occur, if the void volume fraction f takes its ultimate value 1, but much earlier:

$$\Phi(\underline{T}', tr\underline{T}, f, \sigma_m) = \frac{3\,\underline{T}' \cdot\cdot\, \underline{T}'}{2\sigma_m^2} + 2\,q\,f^* \cosh\left(\frac{tr\underline{T}}{2\sigma_m}\right) - 1 - (qf^*)^2 \quad . \tag{3}$$

A typical value for ductile steels is q=1.5 (2). Additionally, Tvergaard and Needleman (2) introduced the modified void volume fraction f^* as

$$f^* = \begin{cases} f & \text{for } f \le f_c \\ f_c + K\,(f - f_c) & \text{for } f > f_c \quad \text{with} \quad K = \dfrac{f_u^* - f_c}{f_f - f_c} \end{cases} \tag{4}$$

considering the coalescence of adjacent voids due to slip planes which occur during the failure process after a critical void volume fraction f_c has been achieved. The crack appears if the final void volume fraction f_f is reached, where the material looses its stress carrying capacity and where the modified void volume fraction f^* achieves its ultimate value f_u^*. The application of these simple micro-mechanical models is justified by a statistical averaging effect over a large number of unit cells on the macroscopic scale. The void evolution consists of two terms, namely the nucleation and growth

$$\begin{aligned} &\dot{f} = \dot{f}_{growth} + \dot{f}_{nucl} \qquad \text{with} \quad \dot{f}_{growth} = (1-f)\,tr\underline{D}^p \\ &\text{and} \quad f(t_0) = f_0 \quad \text{as} \quad \text{initial} \quad \text{condition} \end{aligned} \tag{5}$$

with $\underline{D}^p$ being the plastic part of the strain rate tensor, and f_0 is introduced to be the initial void volume fraction. The evolution equation (5), holding for void growth, is derived by assuming incompressible behaviour of the matrix material (1), while the most difficult modelling problems in the theory of ductile fracture are concerned with the nucleation of micro-voids at the sites of inclusions and second-phase particles in a plastically deforming matrix. An empirical approach for the nucleating part of void evolution written as

$$\dot{f}_{nucl} = A\,\dot{\sigma}_m \quad \text{with} \quad A = \frac{1}{H}\,\frac{f_n}{s_n\sqrt{2\pi}}\,\exp\left(-\frac{1}{2}\left(\frac{\varepsilon_m^p - \varepsilon_n}{s_n}\right)^2\right) \tag{6}$$

was suggested in (5, 6) for strain controlled void nucleation and follows a normal distribution. This strain controlled void nucleation bases on the accumulated plastic strain of the matrix material, ε_m^p. The void volume fraction of void nucleating particles is denoted as f_n, the respective mean critical value is the maximum plastic strain of the void nucleation, ε_n, and s_n is the appropriate standard deviation. The evolution of the yield stress in the matrix material follows the incremental equation

$$\dot{\sigma}_m = H\, \dot{\varepsilon}_m^p \tag{7}$$

where H is the tangent modulus.

DETERMINATION OF MATERIAL PARAMETERS

The material parameters to be determined consist of two classes which characterize the hardening of the matrix material in classical rate independent plasticity and which characterize the evolution of damage in the modified Gurson model. Material hardening for the matrix material in rate independent plasticity is simply characterized by the true stress vs. logarithmic strain curves, $\sigma_m(\varepsilon)$, obtained from uniaxial static tensile and/or compression tests. The damage model described in the previous section includes 7 parameters in total. Three of them (ε_n, s_n, f_n) are used in modelling void nucleation, eqn. (6), and four (q, f_0, f_c, f_f) describe the evolution of void growth up to coalescence and final failure, eqn. (4,5).

The material investigated in the present study is a mild ferritic steel with the German designation StE 460, which contains a lot of perlite islands from which only a part contributes to the nucleation of voids. The determination of that part and of the initial void volume fraction are difficult to perform only by microscopic investigations. In addition to the critical void volume fraction, f_c, and the final void volume fraction, f_f, the initial void volume fraction f_0 was determined numerically, too. The notch radii of the tensile specimens investigated are 4mm and 10mm, respectively. As shown by Tvergaard and Needleman (7), the sudden drop in the load vs. reduction of the diameter curves of the tensile tests, Figs. 1 and 2, is associated with the occurrence of f_c in the centre elements of the bars. Therefore, the load vs. reduction of the diameter curves are used to determine f_0, f_c and f_f by fitting the numerical results into the experimental observations. The stress triaxiality has only a small influence on the critical void volume fraction f_c, as shown by Koplic and Needleman (8) who regarded unit cell models so that the transferability of material parameters obtained from tensile tests to fracture mechanics specimens is ensured.

The parameters were calibrated using the load vs. reduction of diameter data

from the notched tensile bars and determined as: f_0=0.0025, f_c=0.021 and f_f=0.19, Figs. 1 and 2. The results depend not only on the material parameters, but also on the element type and the element sizes in the centre of the bars. In the present investigation, a 4-node linear displacement element with full integration was chosen and the edge length of the centre elements is 0.5mm for the coarse and 0.25mm for the fine mesh, Figs. 1 and 2. Obviously, the smaller elements lead to an earlier failure of the bars caused by an earlier damage of the centre elements. Some further investigations concerning the mesh dependence of results are performed in (9). The simulated load vs. reduction of the diameter curves fit very well in the experimental observations. The material parameters determined and the selected element type are used for all further calculations concerning the steel StE 460. A more detailed description of the method used is given in (10).

SIMULATION OF FRACTURE TESTS

The material parameters obtained from tensile tests of notched bars with different notch radii are used now to predict the ductile crack growth of C(T), M(T) and statically loaded Charpy-V-notched specimens. The C(T) specimens were 25% side grooved and had an initial relative crack length of a/W=0.59. The M(T) specimens were 20% side grooved and their relative initial crack length was a/W=0.49, respectively. The Charpy-V-notched specimens were neither side-grooved nor pre-cracked. The experimental results for the C(T) and M(T) specimens were obtained by the single specimen method with different experiments, Figs. 3, 4 and 5, whereas all experiments for the Charpy-V-notched specimens resulted from the multi specimen method, Figs. 8, 9 and 10.

As a result from the simulation of the experiments using Gurson's model with the material parameters given above, the load vs. displacement curves are shown in Figs. 3 and 4 for the C(T) and for the M(T) specimens. The reference displacements used are the load line displacement, V_{LL}, for the C(T) specimen, and the displacement, V_0, of the point at the specimen's surface about 55mm away from the ligament for the M(T) specimen, respectively. Because plane strain conditions are assumed, the effective thickness of the specimens

$$B_{eff} = \sqrt{B_n \, B} \tag{8}$$

is taken for the calculation of the resulting forces, which leads to the well known fact that the load is overestimated because any 3D effect is neglected. Obviously, the principal behaviour of the load vs. displacement curves is predicted in the right way by a 2D plane strain calculation.

The numerically predicted and the experimentally observed J-resistance curves

are compared in Fig. 5 for the C(T) and M(T) specimens. The steps in the simulated curves are due to the failure of elements in the ligament, i.e., if all integration points in an element reach the final void volume fraction f_f=0.19, the element fails, and crack propagation occurs. The calculations using the Gurson model with one material predict the different behaviour of both specimen geometries within the scattering of the experimental data for the crack initiation as well as for the different slopes during crack propagation parameter set.

A commonly used crack resistance parameter is the crack opening displacement δ_5, first introduced by Schwalbe and Hellmann (11). The appropriate displacements are taken from the FE results and plotted in Fig. 6, where again the steps refer to the failure of elements in the ligament. Obviously, the initiation values depend on the geometry of the specimen as well as the slope of the crack resistance curves. Unfortunately, no experimental data are available for δ_5.

A typical local result is given in Fig. 7 for the C(T) specimen, where the ratio of the crack opening stress to the initial yield stress of the matrix material, σ_{yy}/R_{eL}, from a J-controlled crack propagation analysis using a "sharp" crack is compared to the results from the Gurson calculation. In addition to that, the void volume fraction f ahead of the crack tip is given. The main difference between the crack opening stresses is, that the stresses resulting from the Gurson model decrease to zero ahead of the crack tip indicating that material degradation takes place and the material looses its stress carrying capability. The crack opening stresses are almost identical in the ligament as long as the critical void volume fraction f_c=0.021 is not achieved, Fig. 7. The same material data set is applied to statically loaded Charpy-V-notched specimens. The load vs. displacement of the tup is basically predicted in the right way, Fig. 8, while the overestimation of the force has the same reason as mentioned earlier. The steps in the load vs. displacement curve, Fig. 8, is due to the contact algorithm used at the bearing. The underestimation of the load for larger displacements results from the plane strain model where the constraint in the ligament is overestimated leading to an increasing void growth and crack propagation. The load line displacement vs. crack propagation, Fig. 9, exhibits a large scattering of the experimental data but the prediction with the Gurson model meets the experimental data at an average. The experimental results for the J-integral are obtained according to (12). The numerically predicted results are again within the scattering of the experiments, Fig. 10. The initiation value J_i and the varying slope of the J_R-curve are correctly predicted.

CONCLUSIONS

The modelling of ductile crack growth in ferritic steels using micromechanical models simulates the nucleation, growth and coalescence of voids introducing the

void volume fraction as a damage parameter. Because the micromechanical process is simulated, the material parameters of damage models are independent of the geometry and loading type of the specimens. In the present investigation, Gurson's model is applied, whose material parameters are determined by fitting the numerical results into the experimental observations obtained from tests on notched tensile bars. In a subsequent step, the material parameters obtained are applied to the simulation of C(T), M(T) and statically loaded Charpy-V-notched specimens. It turned out that the usage of one set of material parameters for all types of specimens results in crack resistance curves which are within the scattering of experimental data.

This fact leads to the conclusion, that one set of material parameters has been obtained which really is geometry and loading independent and that Gurson's model is suited to simulate ductile tearing over a wide range of fracture mechanics specimens.

REFERENCES

(1) Gurson, A. L., Journal of Engineering Materials and Technology, Vol. 99, 1977, pp. 2-15.

(2) Needleman, A. and Tvergaard, V., Journal of Mechanics and Physics of Solids, Vol. 32, 1984, pp. 461-490.

(3) McClintock, F. A., Trans. ASME, J. Appl. Mech., Vol. 35, 1968, pp. 363-371.

(4) Rice, J.R. and Tracey, D.M., J. Mech. Phys. Solids, Vol. 17, 1969, pp. 201-217.

(5) Needleman, A. and Rice, J. R., "Limits to ductility by plastic flow localization", Mechanics of Sheet Metal Forming, (eds. D. P. Koistinen and N.-M. Wang), Plenum Publ. Comp. New York, 1978, pp. 237-265.

(6) Chu, C. C. and Needleman, A., J. Engng. Mat. Tech., Vol. 102, 1980, pp. 249-256.

(7) Tvergaard, V. and Needleman, A., Acta Metall., Vol. 32, 1984, pp. 157-169.

(8) Koplic, J. and Needleman, A., Int. J. Solids and Struct., Vol. 24, 1988, pp. 835-853.

(9) Sun, D.-Z., Voss, B. and Schmitt, W., " Numerical prediction of ductile fracture resistance behaviour based on micromechanical models", Defect Assessment in Components - Fundamentals and Applications, ESIS/EGF 9 (Eds. H. Blauel and K.-H. Schwalbe), Mechanical Engineering Publications, London, 1991, 447-458.

(10) Klingbeil, D., Künecke, G. and Schicker, J., "On the application of Gurson´s model to various fracture mechanics specimens", internal Report 93/3 of laboratory 1.31 of the Federal Institute for Materials Research and Testing (BAM), Berlin, 1993.

(11) Schwalbe, K.-H. and Hellmann, D., "Correlation of stable crack growth with the *J*-Integral and the crack tip opening displacement, effects of geometry, size and material", Report GKSS 84/E/37, GKSS-Forschungszentrum Geesthacht, 1984.

(12) Aurich, D. et al., "Analyse und Weiterentwicklung bruchmechanischer Versagenskonzepte - Lokales Rißwachstum, Ermittlung des Rißwiderstandsverhaltens aus der Kerbschlagarbeit", Research Report BAM 192, Federal Institute for Materials Research and Testing (BAM), Berlin (1993). (in German)

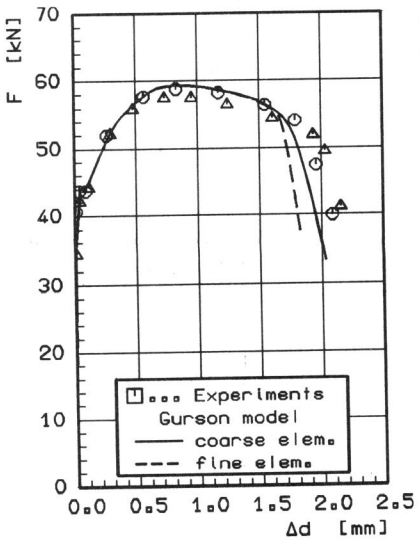

Fig. 1: Load vs reduction of diameter curves for the notched bar, r = 10 mm

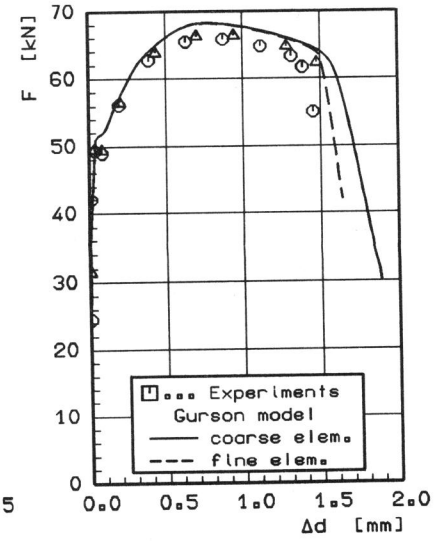

Fig. 2: Load vs reduction of diameter curves for the notched bar, r = 4 mm

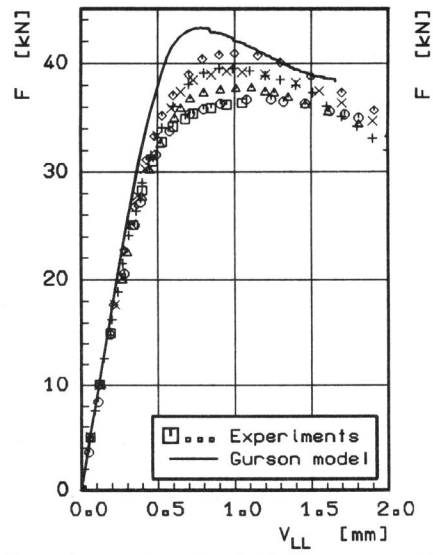

Fig. 3: Load vs load line displacement curves for the C(T) specimen

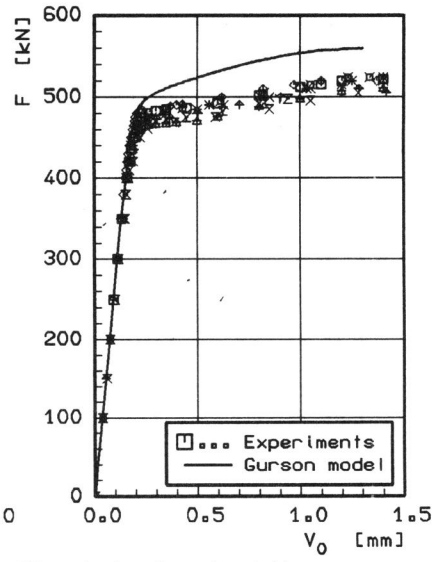

Fig. 4: Load vs load line displacement curves for the M(T) specimen

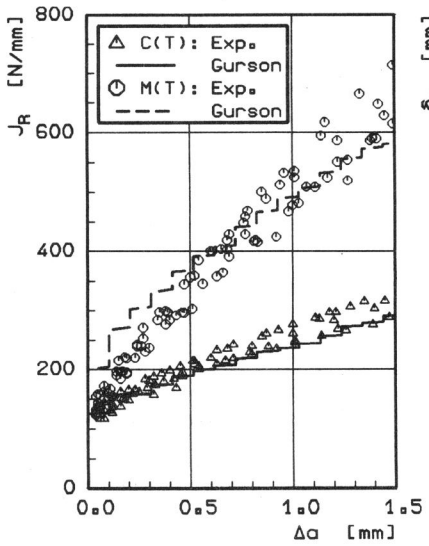

Fig. 5: J_R-curves for C(T) and M(T) specimens

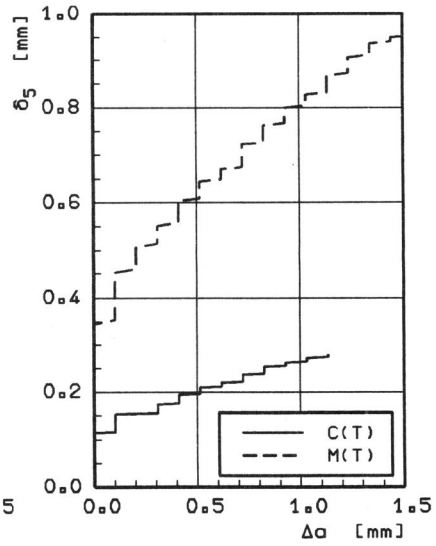

Fig. 6: CTOD resistance curve for C(T) and M(T) specimens

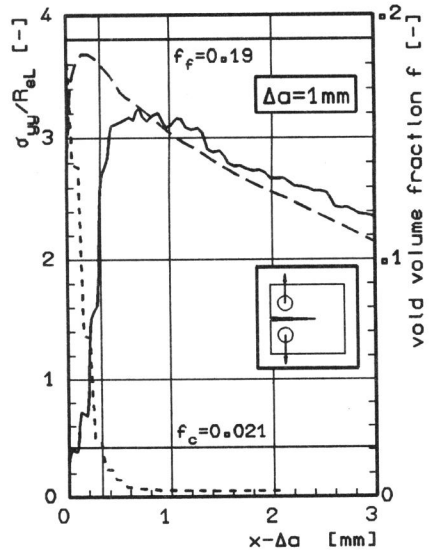

Fig. 7: --- σ_{yy}/R_{eL}, J controlled
—— σ_{yy}/R_{eL}, Gurson model
------ void volume fraction f

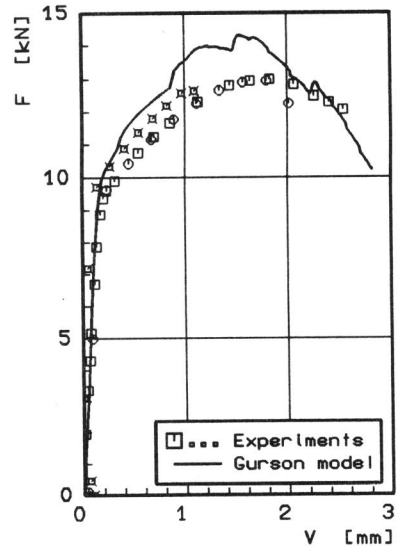

Fig. 8: Load vs load line displacement curve for Charpy-V-notched specimens

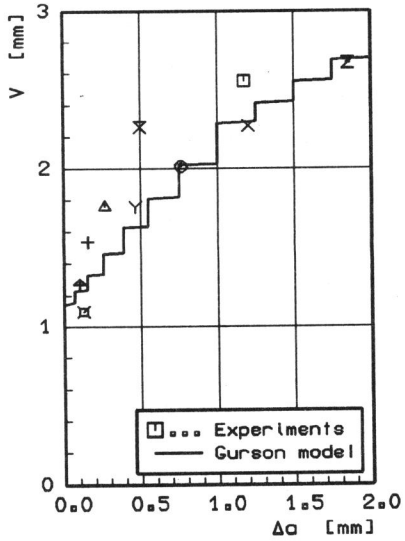

Fig. 9: Load line displacement vs crack propagation for Charpy-V-notched specimens

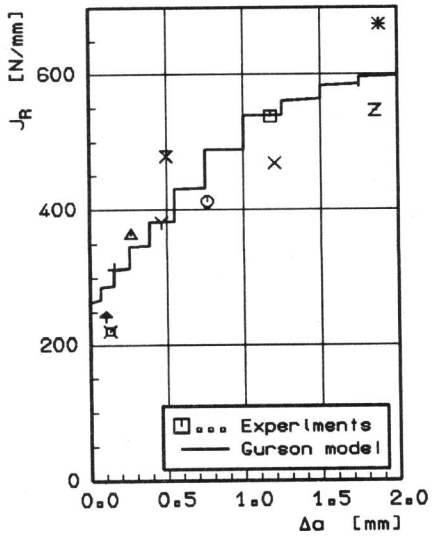

Fig. 10: J_R-curve for the Charpy-V-notched specimen